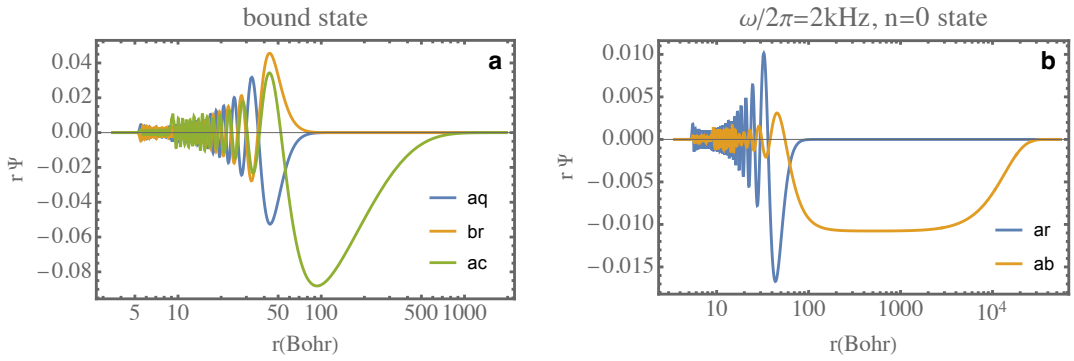

FIG. 2 Example of wave functions from coupled-channels calculations. **(a)** Bound "ac" dimer state. **(b)** Entrance channel "ab" state. There is a 2 kHz harmonic trap added, and this is the lowest-energy state of two atoms interacting at unitarity in the trap.

TABLE I Properties of *ab*-channel wave functions given by Paul. ω is the external trapping potential, $n_{\rm rel}$ is the oscillator number, $f_{\rm cl}$ is the closed-channel fraction, $C_{\rm Np}$ is the contact estimated by Eq. (30), R_* is the characteristic length scale of the closed-channel coupling and caculated using $2\pi f_{\rm cl}/(C_{\rm Np}/N)$ – see Eq. (31), I_d is the dimer overlap, and ℓ_d is the characteristic length scale for the dimer weight, Eq. (34).

$\omega/2\pi$ (kHz)	$n_{\rm rel}$ -	$f_{\rm cl}$ (%)	$C_{\rm Np}/N$ $\times 10^3$, $(1/a_0)$	R_* (a_0)	$C_{\rm Np}/N$ $\times 10^3$, $(1/a_0)$	I_d -	ℓ_d (a_0)
2 kHz	0	0.38%	0.73	33	0.72	0.030	41.7
4 kHz	0	0.55%	1.04	33	1.03	0.043	41.7
8 kHz	0	0.78%	1.47	33	1.47	0.061	41.7
16 kHz	0	1.11%	2.09	33	2.09	0.087	41.6

IV. COUPLED-CHANNELS CALCULATIONS

Paul Julienne has provided wave functions found from coupled-channels calculations at the 202 G Fesbach resonance. These spatial wave functions come decomposed into spin channels; for example *ac*, *aq*, and *br* for the "ac" channel. Data for each spin channel is $u_\alpha(r) = \sqrt{4\pi} r \Psi(r)$, normalized such that $\sum_\alpha \int dr\, |u_\alpha(r)|^2 = 1$. Table I gives some characteristics of the *ab*-channel data provided. Here, $f_{\rm cl}$ is probability weight in the $\alpha = ar$ channel.

In order to test the hypothesis that the dimer-feature weight is proportional to the contact, we need to find the contact for each of the *ab* wave functions provided. One estimate of the contact is (Werner and Castin, 2012), Eq. (31)

$$N_{\rm pair} \sim \frac{C}{4\pi} r \qquad \text{(for small } r\text{)} \tag{27}$$

where $N_{\rm pair}$ is the expectation value for the number of pairs, C is the extensive contact, and r is the inter-particle separation. For the 2-atom case, $N_{\rm pair}$ can only go up to 1. We can find the number of pairs from the open-channel wave function:

$$N_{\rm pair}(r) = \int_0^r dr'\, |u_\alpha(r')|^2 \tag{28}$$

where α is the open-channel spin component, here *ab*. Figure 3(a) shows that we do see this linear behaviour in the wave functions, although with a non-zero intercept. Using the fundamental theorem of calculus, the slope of $N_{\rm pair}$ (and thus the contact) is then

$$C = 4\pi \frac{d}{dr} \int_0^r dr'\, |u_\alpha(r')|^2 = 4\pi |u_\alpha(r)|^2 \tag{29}$$

A comparison of these is shown in Fig. 3(b). We see that the small-r limit seems only satisfied over a small range. In

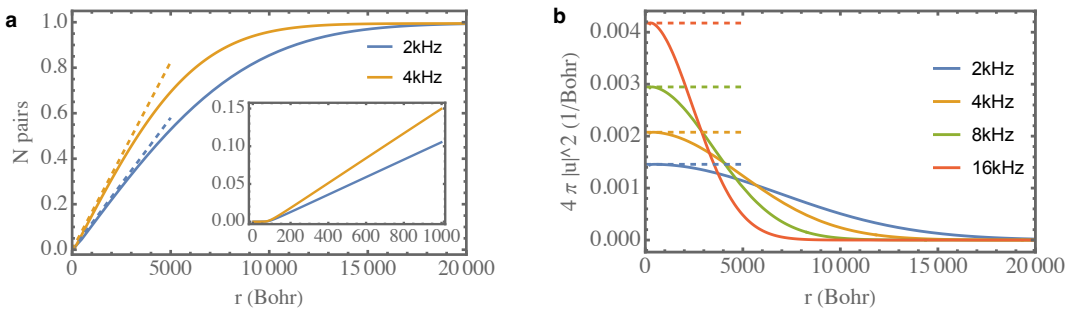

FIG. 3 Finding contact from pair wave functions. **(a)** The expectation value of the number of pairs, found from Eq. (28), versus separation. Dashed lines show the contact, as determined by Eq. (30). Inset: at very short range, the linear increase in probability only begins after some offset. **(b)** $4\pi|u_\alpha(s)|^2$ Dashed lines show the contact, as determined by Eq. (30).

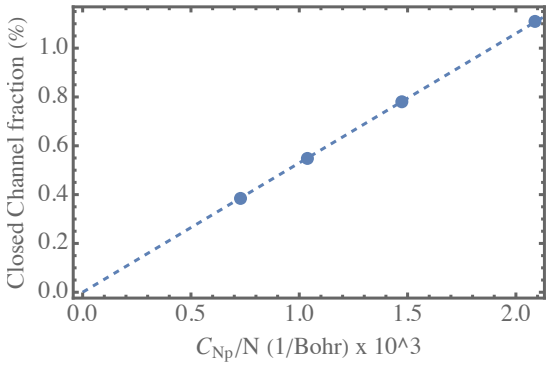

FIG. 4 Closed-channel fraction of pairs at the Feshbach resonance. The closed-channel fraction $f_{\rm cl}$ is plotted versus the contact C_{Np}/N. The dashed line gives the expected slope from Eq. (31), i.e., that $R_* = 33\,a_0$.

practice, we then define the first measure of the contact as

$$C_{\rm Np} \equiv 4\pi \max\{|u_{ab}(r)|^2\} \tag{30}$$

Since this is a two-atom state, we include $C_{\rm Np}/N = C_{\rm Np}/2$ in Table I.

A relation found by Werner, Taurell, and Castin (Werner *et al.*, 2009) is that the closed-channel fraction is proportional to the contact, times a factor that depends on the magnetic moment of the dimer channel. At unitarity, their relation predicts that

$$f_{\rm cl} = \frac{1}{2\pi}\frac{C}{N}R_* \qquad \text{with} \qquad R_* \equiv \frac{\hbar^2}{m a_{\rm bg}\mu_b \Delta B} \tag{31}$$

For the 202 G resonance, $a_{\rm bg} = 167 a_0$, $\mu_b \approx 1.68\mu_B$ (Chin *et al.*, 2010), μ_B is the Bohr magneton, and $\Delta B = 6.9$ G. From these, we find $R_* = 33.3\,a_0$, which explains very well the slope in Fig. 4! Without assuming anything about R_*, we can calculate it from each contact we have found. Alternatively, we can assume R_* is correctly as given, and use the closed-channel fraction to find the contact for each wave function:

$$\frac{C_{\rm R*}}{N} \equiv 2\pi\frac{f_{\rm cl}}{R_*} \tag{32}$$

These are tabulated in Tab. II.

Finally, we come to the dimer feature. The spectral weight of the dimer feature, with a $|b\rangle \to |c\rangle$ spin-flip, is the overlap between the ab initial state and the ac final state:

$$I_d = \left| \int dr\, u^*_{ac}(r) u_{ab}(r) \right|^2 \tag{33}$$

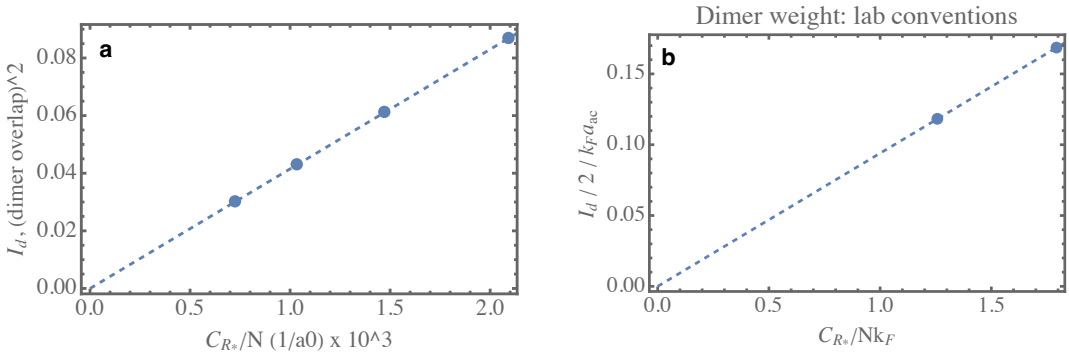

FIG. 5 Dimer feature weight versus contact. (a) The dimer wave function overlap, Eq. (33), is plotted versus contact C/N, determined from the closed-channel fraction of the ac wave function and Eq. (32). The dashed line is Eq. (34) with the best-fit slope, giving a characteristic length $\ell_d = 41(1)\,a_0$. (b) shows this same plot, but in lab units. The value of k_F here corresponds to $E_F/h = 15\,\mathrm{kHz}$, but the slope of this plot is $\ell_d/a_{ac}/2 \approx 0.094$, is independent of k_F. Note the factor of two in the vertical axis, because lab conventions use the sum-rule of 0.5, instead of unity.

These weights are compared to the contact in Fig. 5(a). A clear linear behaviour is shown, with a slope that can be described by a length scale (akin to R_*, but I've taken out the 2π):

$$\boxed{I_d = \ell_d \frac{C}{N}} \tag{34}$$

with $\ell_d \approx 42\,a_0$.

Converting these results to lab conventions, where the rf spectral sum rule is 0.5 instead of unity, we should consider $I_d/2$. Furthermore, we often plot $I_d/2k_F a_{ac}$ versus C/Nk_F. The factors of k_F cancel out of the slope, which is then $\ell_d/(2a_{ac}) \approx 0.094$. See Fig. 5(b).

We can compare the ℓ_d found from this data to the prediction from simple models.

- For a shallow bound state,

$$\ell_d = \frac{1}{\pi} a_{ac} \qquad \text{(shallow dimer state)} \tag{35}$$

  which would give $\sim 71\,a_0$ for $a_{ac} = 222\,a_0$.[2]

- On dimensional grounds, several generalizations might be

$$\ell_d = \frac{1}{\pi}\kappa^{-1} \qquad \text{or} \qquad \ell_d = \frac{1}{\pi}\frac{1}{\kappa^2 a_{ac}} \qquad \text{(dimensionally correct)} \tag{36}$$

  which give $\sim 48\,a_0$ and $\sim 33\,a_0$, respectively. Note that $\kappa^{-1} \approx 151\,a_0$, such that $\kappa a_{ac} \approx 1.5$.

- Including an effective range using a square-well model, and typically assuming $r_e \ll a_{ac}$, one finds

$$\ell_d = \frac{1}{\pi\kappa}\frac{1}{1 + r_e/a_{ac}} \qquad \text{or} \qquad \ell_d = \frac{1}{\pi\kappa}\frac{1}{1 + r_e\kappa} \qquad \text{(square-well model)} \tag{37}$$

  which give $\sim 32\,a_0$ and $\sim 28\,a_0$, respectively, using the closed-channel $r_e = 107\,a_0$. These seem to over-correct for a finite range, but then our experimental scenario, in which $r_e/a_{ac} \approx 0.5$, may exceed the range of validity of the model. Also, note that the the open-channel $(r_e)_{ab} \sim 124\,a_0$, and the models typically use the same effective range for both initial and final channels.

In sum, analytic estimates for ℓ_d range from $28\,a_0$ to $74\,a_0$, bracketing the $42\,a_0$ value found through coupled-channels calculations. A comment on all of the analytical models is that they are for open-channel initial and final states, so we would expect to reduce its prediction for I_d by ∼0.93, the open-channel fraction of the ac channel.

---

[2] Note that the parameterization of the ac scattering length used here ($a_{\mathrm{bg}} = 167.3\,a_0$, $\Delta = 7.2\,\mathrm{G}$, and $B_0 = 224.2\,\mathrm{G}$) has unknown accuracy.